

# Neutrino Mass, Vacuum Stability and Higgs Inflation with Vector-Like Quarks and a Single Right-Handed Neutrino

Canan Karahan\*

*National Defence University, Turkish Naval Academy,  
Department of Basic Sciences, 34942 Tuzla, İstanbul, Türkiye*

We investigate a Standard Model extension containing  $n$  degenerate down-type isosinglet vector-like quarks (VLQs) with masses  $M_{\mathcal{D}}$  and Yukawa couplings  $y_{\mathcal{D}}$ , supplemented by a single right-handed neutrino (RHN), aiming to simultaneously address neutrino mass generation, electroweak vacuum stability, and Higgs inflation. The VLQs play the dominant role in stabilizing the Higgs potential through their impact on the renormalization-group evolution, while the RHN generates light neutrino masses via a Type-I seesaw mechanism and smooths the high-scale running of the Higgs quartic coupling in the inflationary regime. We perform a two-loop Standard Model renormalization-group equation analysis supplemented by the one-loop contributions of the VLQs and the RHN, with proper matching across their mass thresholds. Using these RG trajectories, we identify the regions in  $(n, y_{\mathcal{D}}, M_{\mathcal{D}})$  that stabilize the Higgs potential up to the Planck scale while satisfying experimental constraints. Employing the RG-improved Higgs potential in the metric formulation of non-minimal Higgs inflation, we compute the inflationary observables  $n_s$  and  $r$ . The SM+ $(n)$ VLQ+RHN framework yields predictions consistent with the combined Planck, WMAP, and BICEP/Keck data, while simultaneously ensuring electroweak vacuum stability and phenomenologically viable neutrino masses within well-defined regions of parameter space. For comparison, we also investigate the SM+ $(n)$ VLQ limit and present its vacuum stability and Higgs inflation predictions as a reference to quantify the stabilizing role of the VLQ sector.

---

\* [ckarahan@itu.edu.tr](mailto:ckarahan@itu.edu.tr)

## I. INTRODUCTION

The Standard Model (SM) of particle physics has been remarkably successful in describing a wide range of phenomena. Nevertheless, several experimental observations and theoretical considerations—most notably neutrino masses [1, 2], the metastability of the electroweak vacuum [3, 4], and the need for a viable mechanism for cosmic inflation [5, 6]—point to the need for extensions of the Standard Model. In the following, we briefly discuss these open issues and their implications for physics beyond the Standard Model.

First, neutrino oscillation experiments have established that neutrinos are not massless, contrary to the SM prediction, but have tiny yet finite masses on the sub-eV scale [1, 2]. This calls for an extension of the SM to generate neutrino masses. The most straightforward explanation is the Type-I seesaw mechanism [7–10], which introduces heavy right-handed neutrinos (singlet under SM gauge interactions) that couple to SM lepton doublets. Beside the Type-I seesaw mechanism, there are Type-II [11, 12], Type-III [13] and Type-3/2 [14] seesaw mechanisms, which include a  $SU(2)_L$  triplet scalar field, a  $SU(2)_L$  triplet fermion field and spin-3/2 field, respectively. Among these possibilities, the Type-I seesaw mechanism provides a simple and well-motivated framework for generating light neutrino masses.

Second, the stability of the electroweak (EW) vacuum poses a theoretical puzzle. Given the measured Higgs boson mass  $m_h \approx 125$  GeV and top-quark mass  $m_t \approx 173$  GeV, the RG evolution of the SM couplings to high energies indicates that the Higgs self-coupling  $\lambda_H$  runs to negative values at a scale of order  $10^{10}$  GeV. In other words, the Higgs potential  $V(H)$  develops a second, deeper minimum at high field values, rendering the EW vacuum metastable (with a lifetime longer than the age of the Universe, but not absolutely stable) [3, 4, 15]. This theoretically challenging situation — often called the vacuum stability problem — has been confirmed by high-precision 2-loop [3] and 3-loop [16] computations of the Higgs effective potential. In literature, numerous extensions of the Standard Model have been proposed to address this issue, such as introducing additional scalar fields to raise the Higgs quartic coupling at high energies [17–20], or new fermions/gauge sectors that alter the renormalization-group (RG) running of  $\lambda_H$  [21–23]. In particular, heavy vector-like quarks (VLQs) are an attractive possibility [24, 25]: being color-triplet fermions that receive gauge-invariant mass terms, they are free of gauge anomalies and often appear in extensions like extra-dimensional models or composite Higgs scenarios. A down-type (up-type) isosinglet VLQ (often denoted  $\mathcal{D}$  ( $\mathcal{U}$ ) ) carries the same SM gauge quantum numbers as a right-handed bottom (top) quark (charge  $-1/3$  ( $+2/3$ )), singlet under  $SU(2)_L$  and can mix with the third-generation quarks via its Yukawa interactions. The presence of such a VLQ can modify the RG evolution of  $\lambda_H$ . Notably, if the VLQ has a mass of order the TeV scale and a moderate mixing with the third-generation quarks, it can reduce the effective top Yukawa coupling and strong coupling at high energies, thereby delaying or preventing the eventual turn-over of  $\lambda_H$  to negative values. Indeed, recent studies have shown that the addition of vector-like quarks can stabilize the Higgs potential up to the Planck scale for appropriate parameter choices .

Third, the origin of the cosmic inflationary epoch remains an open question at the intersection of particle physics and cosmology. The simplest models of cosmic inflation postulate a new scalar (inflaton) field to drive exponential expansion in the early Universe [26, 27]. An intriguing alternative is offered by Higgs inflation [28–30]: the identification of the SM Higgs field itself as the inflaton. Higgs field is coupled non-minimally to gravity via a term  $\xi H^\dagger H R$  (where  $R$  is the Ricci scalar curvature and  $\xi$  is a dimensionless coupling). For  $\xi \sim 10^4$ , the Higgs potential in the Einstein frame becomes sufficiently flat at large field values to sustain slow-roll inflation, yielding predictions for the spectral index  $n_s$  and tensor-to-scalar ratio  $r$  in excellent agreement with observations. Higgs inflation is highly economical – it requires no new dynamical degrees of freedom beyond the SM – but its consistency hinges on the stability of the Higgs potential up to the inflationary scales (typically just below the Planck scale). If the potential has a destabilizing turn ( $\lambda_H < 0$ ) at field values below the inflationary plateau, the Higgs field could tunnel to the lower vacuum instead of inflating, ruining the scenario. Ensuring vacuum stability is therefore essential for Higgs inflation to be viable. For the current central values of the Higgs boson mass  $m_h$  and top-quark mass  $m_t$ , the Standard Model alone does not achieve absolute electroweak vacuum stability. This provides strong motivation to consider new physics that can stabilize the Higgs potential and simultaneously allow the Higgs to act as the inflaton.

In this paper, we investigate a minimal phenomenological extension of the SM that addresses all three issues discussed above – neutrino masses, electroweak vacuum stability, and Higgs inflation – in a unified framework. The model introduces just two new sectors of fermionic states: (i) a set of  $n$  degenerate isosinglet down-type VLQs, and (ii) a singlet RHN. The RHN, endowed with a large Majorana mass  $M_N$ , generates light neutrino masses through the Type-I seesaw mechanism and, through its Yukawa coupling, modifies the RG evolution of the Higgs quartic coupling

in the inflationary regime, thereby impacting Higgs inflation <sup>1</sup>The down-type VLQs interact with the SM through the color and hypercharge gauge couplings and via a Yukawa coupling  $y_D$  to the Higgs doublet. For appropriate values of the VLQ mass  $M_D$  and the Yukawa coupling  $y_D$ , these interactions modify the renormalization-group running of the Higgs quartic coupling  $\lambda_H$ , allowing the Higgs potential to remain stable up to the Planck scale. Importantly, this improved stability of the Higgs sector enables successful Higgs inflation: with the addition of RHN and a set of  $n$  degenerate VLQs, the Higgs field can have a stable inflationary potential when coupled to gravity with a non-minimal coupling  $\xi$ , as per the usual Higgs inflation paradigm. In other words, the model simultaneously allows neutrino mass generation (via the seesaw mechanism) and Higgs-driven inflation, while stabilizing the electroweak vacuum. This kind of two-particle type extension of the SM represents a phenomenologically minimalistic yet powerful approach to tackle multiple problems at once, and it remains consistent with current experimental constraints. We emphasize that both new fermions introduced here are singlets under  $SU(2)_L$  and thus do not spoil the  $\rho$ -parameter (custodial symmetry) at tree-level; moreover, being gauge singlets or vector-like, they do not introduce anomalies.

The paper is organized as follows. In Sec.II, we define the particle content and the Lagrangian of the models under consideration, including a detailed description of the Yukawa sector involving the VLQs and the RHN, and we also discuss the relevant parameter space together with the theoretical and experimental constraints imposed on the model. In Sec.III, we investigate the vacuum stability in the presence of the new fermionic degrees of freedom by studying the RG evolution of the Higgs quartic coupling, and we identify the regions of parameter space in which the Higgs potential remains stable up to the Planck scale. In Sec.IV, we study Higgs inflation based on the RG-improved Higgs potential, where the non-minimal coupling  $\xi$  is fixed by the observed amplitude of scalar perturbations and the resulting inflationary predictions are compared with cosmological data. Finally, our conclusions are presented in Sec.V.

## II. MODEL FRAMEWORK

We extend the SM by introducing two additional sectors: (i) a set of  $n$  degenerate down-type isosinglet VLQs, and (ii) a single Majorana RHN. The resulting framework, denoted as  $SM + (n)VLQ + RHN$ , is designed to address three long-standing shortcomings of the SM in a unified manner: the generation of neutrino masses, the stabilization of the electroweak vacuum, and the realization of successful Higgs inflation. For comparison, we also analyze the  $SM + (n)VLQ$  limit obtained by removing the RHN sector, thereby isolating the stabilizing role of the VLQs while excluding the destabilizing contribution of the RHN.

### A. Particle Content and Gauge Representations

The new fields added to the SM are the following:

- Down-type isosinglet vector-like quarks<sup>2</sup>

$$D_{L,R}^{(i)} \sim (3, 1, -1/3), \quad i = 1, \dots, n, \quad (1)$$

transforming as color triplets, electroweak singlets, and hypercharge  $Y = -1/3$ ;

- Majorana right-handed neutrino

$$N \sim (1, 1, 0), \quad (2)$$

which is fully neutral under the SM gauge group.

---

<sup>1</sup> In this work, the RHN is primarily introduced to generate neutrino masses and to affect the renormalization-group evolution of the Higgs sector. A realistic neutrino oscillation pattern would require at least two RHNs, which can be straightforwardly incorporated without affecting our main conclusions.

<sup>2</sup> Up-type vector-like quarks have been extensively studied in the literature, particularly in connection with top partners, but they are typically subject to stronger experimental and theoretical constraints. For this reason, we focus on down-type vector-like quarks in this work.

## B. Lagrangian Structure

### 1. Down-Type Isosinglet Vector-Like Quark Sector

The kinetic and mass terms of down-type isosinglet VLQ sector are

$$\mathcal{L}_D = \overline{D} i \not{D} D - M_D \overline{D} D, \quad (3)$$

where  $M_D$  is a gauge-invariant Dirac mass. For an  $SU(2)_L$  singlet with hypercharge  $Y = -\frac{1}{3}$ , the covariant derivative is  $D_\mu = \partial_\mu - ig_3 T^a G_\mu^a - ig' Y B_\mu$ .

Gauge invariance permits for a single renormalizable Yukawa operator:

$$\mathcal{L}_D^{\text{Yuk}} = -y_D \overline{Q}_L H \mathcal{D}_R + \text{h.c.}, \quad (4)$$

where  $Q_L$  is the SM quark doublet and  $H$  is the usual Higgs doublet. In the following, we assume that the down-type VLQs couple only to the third-generation Standard Model quarks. This choice suppresses potentially dangerous flavor-changing neutral currents and is consistent with current experimental bounds. For RG evolution we assume all VLQs to be mass and Yukawa coupling degenerate:

$$M_D^{(i)} = M_D, \quad y_D^{(i)} = y_D. \quad (5)$$

### 2. Right-Handed Neutrino Sector

The RHN kinetic and Majorana mass terms are

$$\mathcal{L}_N = \frac{1}{2} \overline{N} i \not{D} N - \frac{1}{2} M_N \overline{N}^c N. \quad (6)$$

The neutrino Yukawa interaction is

$$\mathcal{L}_N^{\text{Yuk}} = -y_N \overline{L} \tilde{H} N + \text{h.c.}, \quad (7)$$

producing a Dirac mass  $m_D = y_N v / \sqrt{2}$  after electroweak symmetry breaking. Here,  $\tilde{H} \equiv i\sigma_2 H^*$  denotes the  $SU(2)_L$ -conjugate Higgs doublet.

A light neutrino mass arises from the Type-I seesaw mechanism:

$$m_\nu = \frac{y_N^2 v^2}{2M_N}. \quad (8)$$

## C. Parameter Space and Model Limits

The full parameter set of the extended model is

$$\{n, M_D, y_D, M_N, y_N\}. \quad (9)$$

To reproduce the characteristic light-neutrino mass scale  $m_\nu \simeq 0.05$  eV indicated by oscillation data [2, 31, 32], we fix the right-handed neutrino parameters to the values<sup>3</sup>

$$M_N \simeq 10^{14} \text{ GeV}, \quad y_N \simeq 0.42, \quad (10)$$

which yield the correct order of magnitude for the Type-I seesaw relation Eq.(8). With the neutrino sector thus fixed, the remaining free parameters of the model reduce to the three-dimensional set  $\{n, M_D, y_D\}$ , which fully determines the vacuum stability and Higgs-inflation phenomenology studied in the following sections. An upper bound  $n \leq 10$  is imposed by the requirement of perturbativity of the strong gauge coupling. Beyond this value, the cumulative contribution of the VLQs to the QCD beta function drives  $g_3$  into the non-perturbative regime at scales relevant for vacuum stability and Higgs inflation. From this point onward, we present our analysis under two model frameworks: the full  $SM + (n)VLQ + RHN$  scenario and its  $SM + (n)VLQ$  limit, in which the right-handed neutrino sector is removed.

<sup>3</sup> These values are not only consistent with neutrino oscillation data, they are also chosen such that the RHN sector plays an active role in shaping the RG evolution of the Higgs quartic coupling.

## D. Experimental and Theoretical limits

### 1. Experimental constraints on the Yukawa coupling $y_D$ and mass $M_D$

In the SM extended by down-type isosinglet VLQs with the mass  $M_D$  and Yukawa interaction  $y_D$ , the mass terms after electroweak symmetry breaking lead to a left-handed mixing angle defined by

$$\sin \theta_L \simeq \frac{y_D v}{\sqrt{2} M_D}, \quad (11)$$

where  $v \simeq 246$  GeV is the Higgs vacuum expectation value. This relation follows from the standard diagonalization of the VLQ-SM mass matrix and is consistent with the formalism developed in vector-like quark studies [36, 37].

Current LHC searches set stringent lower bounds on the mass of down-type singlet VLQs. ATLAS Run 2 pair-production analyses exclude  $M_D \lesssim 1.3$  TeV in the singlet- $\mathcal{D}$  [33], while the most recent CMS search at  $\sqrt{s} = 13$  TeV with  $138 \text{ fb}^{-1}$  further strengthens this limit by excluding  $M_D \lesssim 1.5$  TeV at 95% C.L. [34]. These results, representative of the latest ATLAS and CMS constraints on pair-produced singlet VLQs, consistently indicate that masses below the  $\sim 1.5$  TeV range are ruled out.

In addition to the mass bounds, the mixing of a down-type singlet vector-like quark with the SM bottom quark is strongly constrained by electroweak precision data. Such mixing induces a tree-level modification of the  $Z\bar{b}b$  couplings, approximately given by  $\delta g_L^b \simeq -\theta_L^2$ . The excellent agreement between the LEP/SLC measurements and the Standard Model predictions, therefore, allows only tiny deviations. Global fits to the Z-pole observables consequently constrain the left-handed mixing angle to the percent level,  $|\sin \theta_L| \lesssim \mathcal{O}(10^{-2})$ , almost independently of the VLQ mass. This conclusion has been consistently confirmed in modern analyses of VLQ mixing [35–37].

In light of these constraints, and to ensure full compatibility with current experimental data, we adopt a conservative benchmark setup for our numerical analysis. In particular, the VLQ Yukawa coupling  $y_D$  is considered within a range such that the induced left-handed mixing angle remains in the experimentally allowed regime at the level of  $\mathcal{O}(10^{-2})$ , consistent with bounds from electroweak precision observables. Furthermore, we impose a lower bound on the VLQ mass,  $M_D \gtrsim 1.5$  TeV, consistent with current LHC searches.

### 2. Theoretical constraints on the Yukawa coupling $y_D$

In addition to the experimental limits discussed above, the down-type VLQ Yukawa coupling  $y_D$  is subject to several theoretical consistency conditions. These constraints ensure that the theory remains perturbative, unitary, and free of Landau poles up to the Planck scale.

*a. Perturbativity and Landau-pole constraints* The Yukawa interaction Eq.(4) of the down-type VLQ is subject to theoretical consistency requirements that limit its viable parameter range. These conditions ensure the perturbative validity of the theory and prevent the appearance of ultraviolet Landau singularities.

The perturbative expansion demands

$$|y_D| \lesssim \sqrt{4\pi}. \quad (12)$$

In practice, phenomenological analyses of VLQ models commonly impose a stronger requirement,  $|y_D| \lesssim 1$ , to avoid rapid growth of the cubic term in the beta function,

$$\beta_{y_D} \sim \frac{y_D^3}{16\pi^2},$$

which is known to dominate the running at large Yukawa couplings. This bound ensures that perturbativity is maintained over the entire range of scales relevant for our RGE evolution.

Above the VLQ mass threshold,  $\mu \simeq M_D = \mathcal{O}(\text{TeV})$ , the Yukawa coupling becomes active in the renormalization-group evolution and starts to run according to the full SM+ $n$ VLQ+RHN beta function. The growth is accelerated by the cubic  $y_D^3$  term, and sufficiently large values of  $y_D$  at the matching scale can drive the coupling to a Landau pole far below the Planck scale. Requiring the absence of a Landau pole below the Planck scale and the validity of perturbation theory up to the scales relevant for electroweak vacuum stability and Higgs inflation therefore imposes a

stringent upper bound on the VLQ Yukawa coupling. To remain safely within the perturbative regime, we therefore adopt the following conservative benchmark

$$|y_D| \lesssim 0.5, \quad (13)$$

where the precise bound depends on the number of VLQs and the scale up to which perturbativity is required. Larger values typically lead to a rapid loss of perturbative control once renormalization-group effects are taken into account [38].

These constraints guarantee that the Yukawa sector remains under perturbative control from the VLQ threshold up to the ultraviolet scales probed in our vacuum-stability and Higgs-inflation analysis.

*b. Tree-level unitarity.* Perturbative unitarity of the  $2 \rightarrow 2$  scattering amplitudes places an additional theoretical bound on the eigenvalues of the Yukawa interaction matrix. Adopting the standard partial-wave unitarity condition for  $s$ -wave amplitudes, as commonly employed in the literature [39, 40], we require that all such amplitudes satisfy the condition  $|a_0| < 1$ , which implies, for a single down-type VLQ,

$$|y_D| \lesssim \sqrt{8\pi} \quad (14)$$

which is considerably weaker than the perturbativity and Landau pole limits discussed above. This bound nonetheless defines the absolute perturbative domain of the theory.

The vacuum-stability requirement, in contrast, yields a far stronger restriction on  $y_D$  through its renormalization-group effects on the Higgs quartic coupling. Since vacuum stability constitutes a central part of our analysis, the full RGE-based stability conditions—together with the experimental and theoretical constraints discussed above—are examined in detail in the following section.

### III. VACUUM STABILITY ANALYSIS

The scale dependence of the Higgs quartic coupling  $\lambda(\mu)$  is governed by the RGEs presented in Appendix A. For numerical integration, all SM couplings are initialized at the top-quark mass scale  $\mu = m_t$  using the input values listed in Appendix B. In the SM, the large top Yukawa coupling drives  $\lambda(\mu)$  negative around  $\mu \sim 10^{10}$  GeV when the Higgs and top-quark masses are set to their current central values,  $m_h \simeq 125$  GeV and  $m_t \simeq 173$  GeV [4, 31]. Both the down-type vector-like quark (VLQ) sector and the right-handed neutrino (RHN) affect this running: VLQs contribute *positively* to  $\beta_\lambda$ , while the RHN contributes *negatively*. The vacuum stability of the model therefore depends sensitively on the VLQ Yukawa coupling  $y_D$ , the number of VLQs  $n$ , and the VLQ mass threshold  $M_D$ .

#### A. Vacuum Stability in the $SM + (n)VLQ + RHN$ Framework

We solve the coupled RGEs from the electroweak scale up to the Planck scale using one-loop BSM contributions and two-loop SM contributions. The effective VLQ threshold is implemented at  $\mu = M_D$ , at which the matching conditions for gauge, Yukawa and quartic couplings are applied. The RHN threshold is fixed at  $M_N = 10^{14}$  GeV.

First, for each parameter point  $(n, y_D, M_D)$  we evolve the RGEs up to the Planck scale and determine the minimum value of the running Higgs quartic coupling,

$$\lambda_{\min} \equiv \min_{\mu \leq M_{\text{Pl}}} \lambda(\mu). \quad (15)$$

By scanning over  $y_D$  for fixed  $(n, M_D)$ , we identify the critical value at which  $\lambda(\mu)$  first becomes negative, thereby determining the boundary beyond which vacuum stability is lost. Points with  $\lambda_{\min} > 0$  indicate an absolutely stable electroweak vacuum, while  $\lambda_{\min} < 0$  corresponds to a metastable or unstable vacuum, depending on whether the tunneling lifetime exceeds the age of the Universe.

Fig.1 illustrates the vacuum-stability properties of the  $SM + (n)VLQ + RHN$  framework. Each panel shows the minimum value of the Higgs quartic coupling,  $\lambda_{\min}$ , as a function of the VLQ Yukawa coupling  $y_D$  for  $n = 1-10$  and for the benchmark masses  $M_D = 1.5, ; 3.0, ; 5.0$  TeV, respectively. In all cases, the RHN Yukawa coupling is fixed to  $y_N = 0.42$ <sup>4</sup>.

<sup>4</sup> Throughout this work, the Yukawa couplings  $y_D$  and  $y_N$  denote the input values defined at their respective mass thresholds,  $y_D(M_D)$  and  $y_N(M_N)$ , and are evolved according to the renormalization-group equations above these scales.

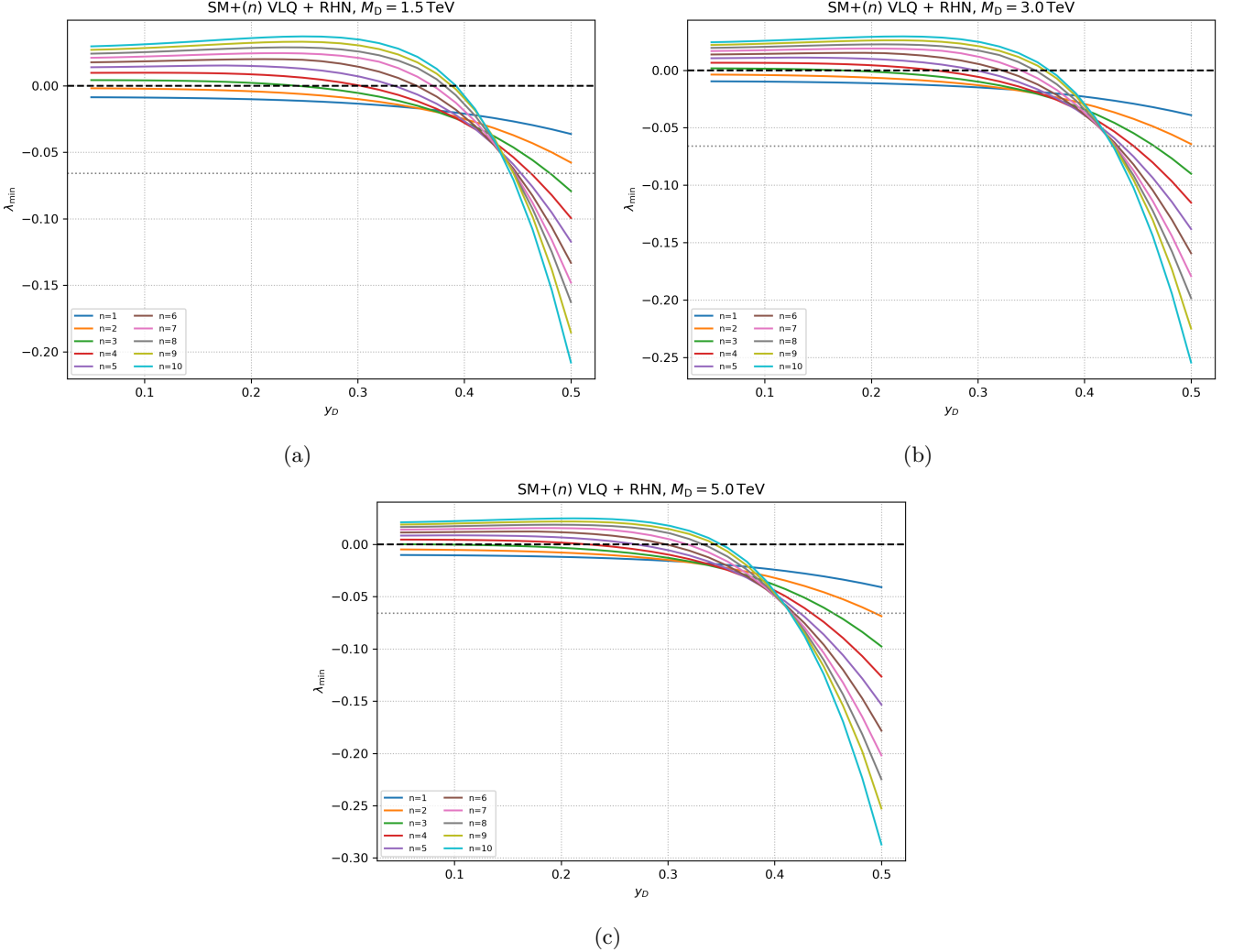


FIG. 1. Vacuum stability in the SM+(n) VLQ+RHN framework. Panels (a)–(c) show the minimum value  $\lambda_{\min}$  as a function of the VLQ Yukawa coupling  $y_D$  for benchmark masses  $M_D = 1.5, 3.0, 5.0$  TeV, respectively. In each panel, curves correspond to  $n = 1\text{--}10$ .

The behavior of the curves determines which combinations of  $(n, y_D, M_D)$  lead to a stable electroweak vacuum. The main features of Fig.1 can be summarized as follows:

1. For fixed values of  $(n, M_D)$ , the minimum value of the Higgs quartic coupling,  $\lambda_{\min}$ , exhibits a monotonic decrease as the VLQ Yukawa coupling  $y_D$  is increased. The point at which a given trajectory intersects the line  $\lambda_{\min} = 0$  signals the onset of vacuum instability for the corresponding  $(n, M_D)$ . Parameter regions with  $\lambda_{\min} > 0$  correspond to an absolutely stable electroweak vacuum, whereas  $\lambda_{\min} < 0$  indicates a metastable or unstable Higgs potential.
2. Comparing the three panels, the range of Yukawa couplings  $y_D$  that keeps  $\lambda_{\min} > 0$  becomes more restrictive as VLQ mass  $M_D$  increase.
3. At all three benchmark masses, the dependence on the number of VLQs  $n$  shows a characteristic two-regime behaviour. For sufficiently small Yukawa couplings, increasing  $n$  shifts  $\lambda_{\min}$  upward and improves vacuum stability. However, beyond a certain  $y_D$  value in each panel, the destabilizing  $\sim -n y_D^4$  contribution dominates the running, and the trend reverses: larger  $n$  then drives  $\lambda_{\min}$  downward more rapidly as  $y_D$  increases. This turnover is clearly visible in all three plots and marks the point beyond which the number of VLQs  $n$  no longer stabilizes the vacuum but instead accelerates its loss.
4. In particular, the case  $n = 1$  and  $n = 2$  never yields a stable electroweak vacuum for any of the benchmark

masses. For  $n \geq 3$ , vacuum stability can be achieved within a finite interval of small  $y_D$ , but this interval becomes progressively narrower as  $M_D$  is increased.

Taken together, these results show that, in the presence of a single RHN with  $y_N = 0.42$ , restoring vacuum stability requires sufficiently small VLQ Yukawa couplings and, in practice, at least three or more down-type VLQs, with the case  $n = 3$  being viable only for the benchmark masses  $M_D = 1.5, 3.0$  TeV.

To illustrate the scale evolution of the Higgs quartic coupling more transparently, we select a common Yukawa value for all benchmark masses. Since vacuum stabilization with the smallest possible number of VLQs is achieved only in the region of relatively small VLQ Yukawa couplings, we adopt a conservative choice  $y_D = 0.15$ . This value lies within the experimentally allowed region for all benchmark masses according to Eq.(11) and ensures that the stabilizing effect of the VLQ sector can already be realized for the minimal viable  $n$ , enabling a meaningful comparison of the running of  $\lambda(\mu)$  as a function of the number of VLQs.

The running of the Higgs quartic coupling as a function of the renormalization scale is presented in Fig.(2) for the benchmark VLQ mass values  $M_D = 1.5, 3.0, 5.0$  and 5 TeV.

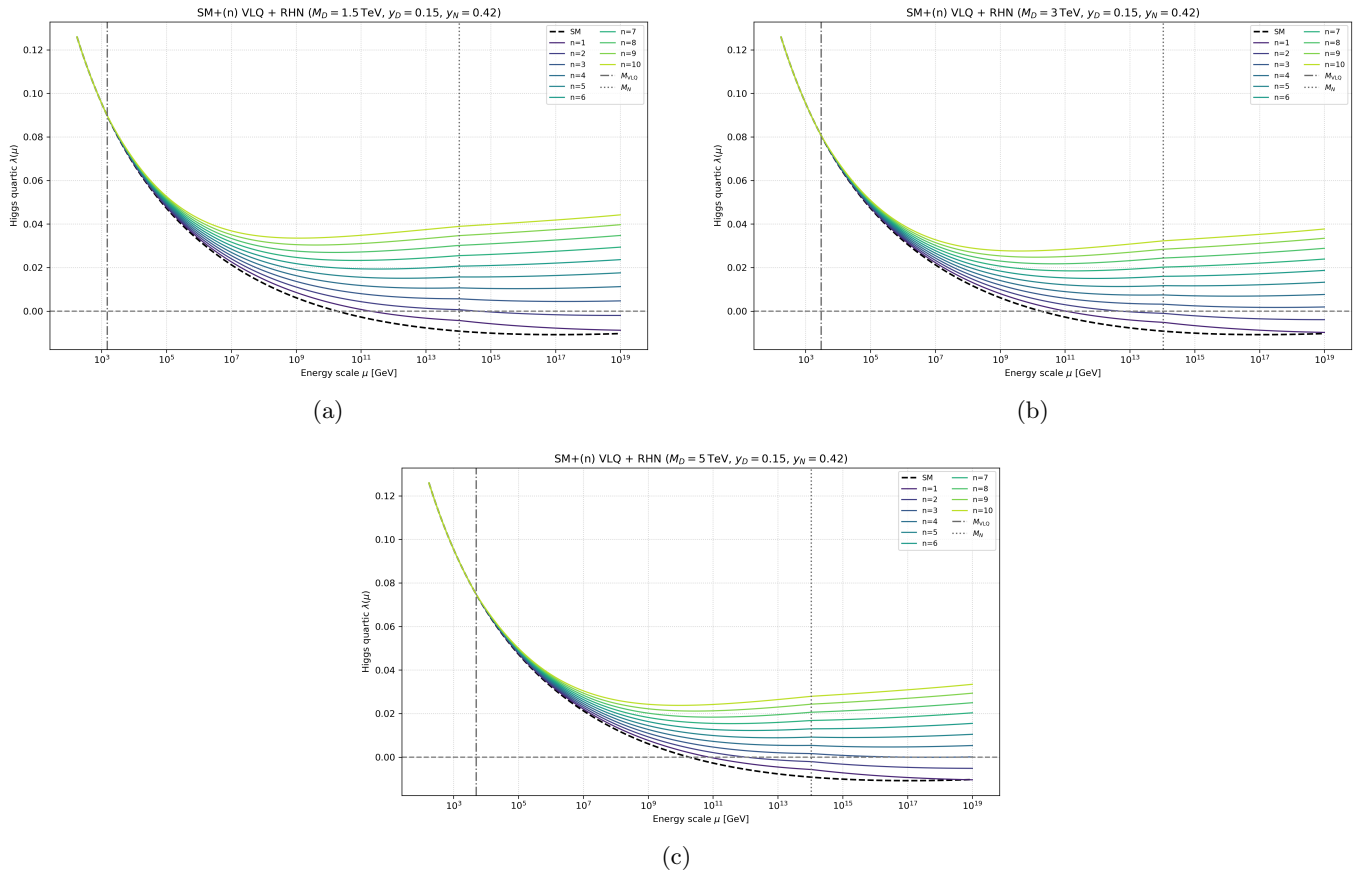


FIG. 2. Running of the Higgs quartic coupling  $\lambda(\mu)$  in the SM+(n)VLQ+RHN model for the benchmark VLQ masses  $M_D = 1.5, ; 3.0, ; 5.0$  TeV. The curves correspond to  $n = 1-10$  for fixed  $y_D = 0.15$  and  $y_N = 0.42$ , while the dashed black curve shows the SM result. The vertical dashed and dotted lines indicate the VLQ and RHN mass thresholds, respectively.

As indicated by the stability limits in Fig.1, the case  $n = 1$  and  $n = 2$  fail to stabilize the Higgs potential for any of the benchmark masses considered, while  $n = 3$  achieves stability only for  $M_D = 1.5$  and 3.0 TeV. In contrast, for  $n \geq 4$  all three benchmark mass values successfully maintain a positive Higgs quartic coupling up to the Planck scale. Fig. (2) further illustrates this behavior: as the number of VLQs  $n$  increases, their contribution to the RG evolution shifts the running of  $\lambda(\mu)$  toward larger values, such that the Higgs quartic coupling remains positive up to the Planck scale.

Moreover, the evolution of  $\lambda(\mu)$  in the inflationary domain  $10^{15} - 10^{19}$  GeV remains remarkably smooth, with no indication of rapid variations or destabilizing trends. This controlled high-scale behaviour reflects a well-balanced interplay between the destabilizing RHN Yukawa contribution and the stabilizing effect of the VLQ sector. Such mild running of the quartic coupling is precisely the regime required for a viable Higgs-inflation setup, where the flatness and stability of the effective potential are sensitive to the ultraviolet behaviour of  $\lambda(\mu)$ .

## B. Vacuum Stability in the $SM + (n)VLQ$ Framework

In the absence of RHN, the stabilizing effect of the VLQs is significantly stronger: the allowed region in  $y_D$  is wider and the values of  $\lambda_{\min}$  are consistently higher. This comparison highlights the non-trivial impact of individual fermionic degrees of freedom on the high-scale behavior of the effective potential.

Following the same procedure as in the  $SM + (n)VLQ + RHN$  framework discussed in the previous section, we analyze the dependence of Higgs vacuum stability on the VLQ Yukawa coupling  $y_D$ . For the benchmark masses  $M_D = 1.5, 3.0, 5.0$  TeV, the RGEs are evolved up to the Planck scale, and the corresponding minimum value of the Higgs quartic coupling,  $\lambda_{\min}$ , is extracted.

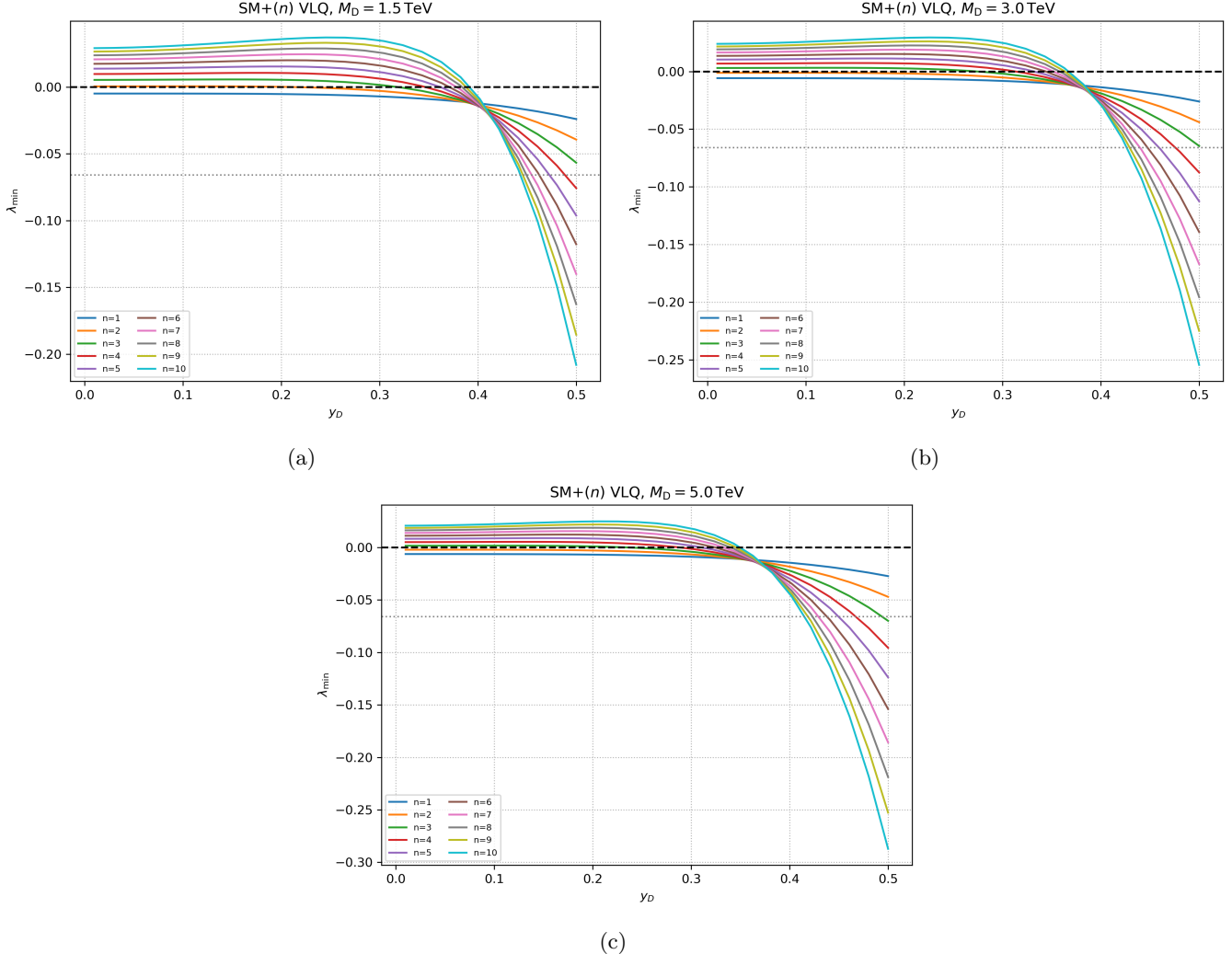


FIG. 3. Vacuum stability in the  $SM + (n) VLQ$  framework. Panels (a)–(c) show the minimum value  $\lambda_{\min}$  as a function of the VLQ Yukawa coupling  $y_D$  for benchmark masses  $M_D = 1.5, 3.0, 5.0$  TeV, respectively. In each panel, curves correspond to  $n = 1-10$ .

Fig.3 displays the minimum value of the Higgs quartic coupling,  $\lambda_{\min}$ , as a function of the VLQ Yukawa coupling  $y_D$ , for  $n = 1-10$  and for the benchmark mass choices  $M_D = 1.5, 3.0, 5.0$  TeV. Compared with the  $SM + (n) VLQ + RHN$  case discussed previously, the qualitative behaviour remains similar, but important differences appear because the destabilizing RHN Yukawa contribution is now absent. The main features of Fig.3 can be summarized as follows:

1. Removing the RHN Yukawa eliminates the negative contribution that previously pushed  $\lambda_{\min}$  downward at high scales. Consequently, for each  $n$ ,  $\lambda_{\min}$  stays higher than in the full  $SM + (n) VLQ + RHN$  model. This confirms that VLQs alone have a net stabilizing tendency at small Yukawa couplings.
2. As in the full model, increasing the number of VLQs shifts the running upward, delaying (or preventing) the

point at which  $\lambda_{\min}$  turns negative. However, without the RHN, this stabilizing effect is stronger and persists to larger values of  $y_D$ .

3. The characteristic transition seen previously — where large values of  $n$  eventually accelerate the fall of  $\lambda_{\min}$  still appears, but with a reduced rate and at later scales. In other words, the destabilizing regime sets in more softly because only the VLQ sector drives it, not the RHN.
4. In the SM+ $(n)$ VLQ+RHN case,  $n = 1$  and  $n = 2$  never achieved stability in the allowed parameter space. Here, for SM+ $(n)$ VLQ, even small  $n$  values lead to a visibly less negative  $\lambda_{\min}$ , and several trajectories remain close to or above zero. For  $n = 2$ , a vacuum-stable region exists only for the lightest VLQ mass  $M_D = 1.5$  TeV, while for  $M_D = 3.0$  and 5.0 TeV the  $n = 2$  curve stays in the metastable regime. Models with  $n \geq 3$  are substantially more stable than in the full model, confirming that the RHN Yukawa was the primary destabilizing agent.
5. Overall, the SM+ $(n)$ VLQ scenario leads to improved electroweak vacuum stability compared to the SM+ $(n)$ VLQ +RHN model for all considered values of  $n$  and  $M_D$ , as reflected by larger values of  $\lambda_{\min}$  and a broader region with  $\lambda_{\min} > 0$ . In this case, vacuum stability is still governed primarily by the interplay between  $n$  and  $y_D$ . The absence of the RHN Yukawa contribution generally enlarges the stability region, particularly for larger values of  $n$ .

To illustrate the scale dependence of the Higgs quartic coupling in a transparent manner, we fix the VLQ Yukawa coupling to a common benchmark value,  $y_D = 0.15$ , for all considered VLQ masses. The resulting running of the Higgs quartic coupling,  $\lambda(\mu)$ , is shown in Fig.4 for the benchmark masses  $M_D = 1.5, 3.0, 5.0$  TeV.

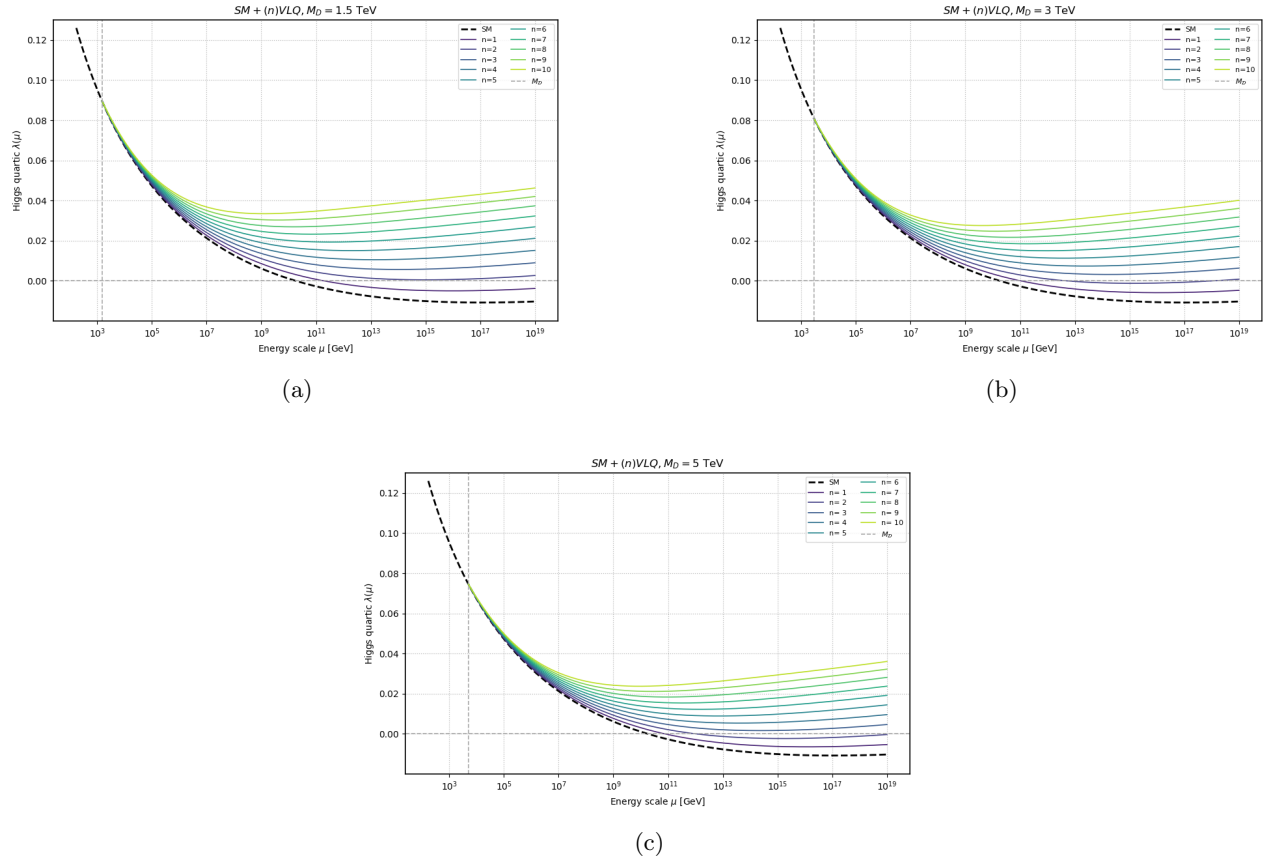


FIG. 4. Running of the Higgs quartic coupling  $\lambda(\mu)$  in the SM+ $(n)$ VLQ framework for the benchmark VLQ masses  $M_D = 1.5, ; 3.0, ; 5.0$  TeV. The curves correspond to  $n = 1-10$  for fixed  $y_D = 0.15$ , while the dashed black curve shows the SM result. The vertical dashed line indicates the VLQ mass threshold.

As seen from the Fig.4, the cases  $n = 1$  is insufficient to stabilize the Higgs potential for any of the benchmark masses considered, while  $n = 2$  leads to vacuum stability only for the lower mass values  $M_D = 1.5$  TeV. For  $n \geq 3$ , all benchmark masses yield a positive Higgs quartic coupling up to the Planck scale.

In comparison with the full SM+ $(n)$ VLQ+RHN framework, the SM+ $(n)$ VLQ model exhibits a noticeably different high-scale behaviour. Although the addition of VLQs alone lifts the running of  $\lambda(\mu)$  and delays the destabilization of the potential, the quartic coupling develops an enhanced curvature at intermediate and high scales. By contrast, the SM+ $(n)$ VLQ+RHN scenario displays a remarkably smooth evolution of  $\lambda(\mu)$  throughout the inflationary domain  $10^{15}$ – $10^{19}$  GeV. This smoothness does not arise from the VLQ contribution alone; rather, it is a consequence of the delicate balance between the stabilizing effect of the VLQ sector and the destabilizing RHN Yukawa interaction. These competing contributions partially cancel, yielding a controlled and slowly varying high-scale running of the quartic coupling with no abrupt changes in slope. Such regulated ultraviolet behaviour is precisely the regime required for a viable Higgs–inflation setup, where the flatness and stability of the effective potential are highly sensitive to the evolution of  $\lambda(\mu)$ .

In the SM+ $(n)$ VLQ+RHN framework, the absence of this balancing mechanism leads to a less regulated high-scale trajectory. While the vacuum–stability region is generally enlarged once the RHN contribution is removed, the smooth inflationary behaviour characteristic of the full SM+ $(n)$ VLQ+RHN model is no longer reproduced.

These vacuum stability results provide the foundation for the Higgs inflation analysis in Sec. IV, where the requirement of a positive RG-improved quartic coupling plays a central role in determining the inflationary potential.

#### IV. HIGGS INFLATION

In our framework the radial mode of the Standard Model Higgs doublet plays the role of the inflaton at large field values. The Higgs field is non-minimally coupled to gravity in the metric formulation via

$$S \supset \int d^4x \sqrt{-g} \left[ -\frac{M_{\text{Pl}}^2}{2} R - \xi H^\dagger H R + (D_\mu H)^\dagger (D^\mu H) - V(H, \mu) \right], \quad (16)$$

where  $M_{\text{Pl}}$  is the reduced Planck mass,  $\xi$  is the non-minimal Higgs–gravity coupling, and  $V(H, \mu)$  denotes the renormalization-group (RG) improved Higgs potential. Working in unitary gauge and denoting the real Higgs field by  $\phi$ , we write the Jordan-frame potential as

$$V_J(\phi, \mu) = \frac{1}{4} \lambda(\mu) \phi^4, \quad (17)$$

where  $\lambda(\mu)$  is the running Higgs quartic coupling obtained from the full two-loop SM RGEs supplemented by the one-loop contributions of the vector-like quarks and the right-handed neutrino, with appropriate threshold matching at  $\mu = M_D$  and  $\mu = M_N$ . In the inflationary regime we employ the usual approximation

$$\mu \simeq \phi, \quad (18)$$

so that the RG-improved potential is evaluated self-consistently along the inflaton trajectory. We restrict the analysis to the field range where  $\lambda(\phi) > 0$  and  $\phi$  lies between  $10^{15}$  GeV and  $10^{19}$  GeV.

To study inflation, we perform a Weyl rescaling to the Einstein frame,

$$g_{\mu\nu} \rightarrow \tilde{g}_{\mu\nu} = \Omega^2(\phi) g_{\mu\nu}, \quad \Omega^2(\phi) = 1 + \xi \frac{\phi^2}{M_{\text{Pl}}^2}, \quad (19)$$

which yields a canonical Einstein–Hilbert term and an effective scalar potential

$$U(\phi) = \frac{\lambda(\phi)}{4} \frac{\phi^4}{(1 + \xi \phi^2/M_{\text{Pl}}^2)^2}. \quad (20)$$

Due to the non-minimal coupling, the kinetic term of  $\phi$  becomes non-canonical in the Einstein frame. Introducing a canonically normalized field  $\chi$  via

$$\frac{d\chi}{d\phi} = \sqrt{\frac{1 + \xi(1 + 6\xi)\phi^2/M_{\text{Pl}}^2}{(1 + \xi\phi^2/M_{\text{Pl}}^2)^2}}, \quad (21)$$

we can express the slow-roll dynamics in terms of the Einstein-frame potential  $U$  as a function of  $\chi$ .

In the slow-roll approximation, the relevant parameters are

$$\epsilon(\chi) = \frac{M_{\text{Pl}}^2}{2} \left( \frac{1}{U} \frac{dU}{d\chi} \right)^2, \quad (22)$$

$$\eta(\chi) = M_{\text{Pl}}^2 \frac{1}{U} \frac{d^2U}{d\chi^2}. \quad (23)$$

For numerical convenience we evaluate the derivatives with respect to  $\phi$  and use the chain rule. Defining  $U'(\phi) \equiv dU/d\phi$  and  $\chi'(\phi) \equiv d\chi/d\phi$ , we have

$$\frac{dU}{d\chi} = \frac{U'(\phi)}{\chi'(\phi)}, \quad (24)$$

$$\frac{d^2U}{d\chi^2} = \frac{1}{\chi'(\phi)} \frac{d}{d\phi} \left( \frac{dU}{d\chi} \right) = \frac{1}{\chi'(\phi)} \frac{d}{d\phi} \left( \frac{U'(\phi)}{\chi'(\phi)} \right). \quad (25)$$

The end of inflation is determined by the condition

$$\epsilon(\phi_{\text{end}}) = 1, \quad (26)$$

which implicitly defines  $\phi_{\text{end}}$  (and the corresponding  $\chi_{\text{end}}$ ). The number of e-folds between a generic field value  $\phi$  and the end of inflation is given by

$$N(\phi) = \int_{\phi_{\text{end}}}^{\phi} \frac{U(\varphi)}{U'(\varphi)} \frac{\chi'(\varphi)^2}{M_{\text{Pl}}^2} d\varphi, \quad (27)$$

which we evaluate numerically using a trapezoidal integration over the  $\phi$  grid. For a given target value  $N_*$  (typically  $N_* \simeq 55$ ), the field value at horizon exit,  $\phi_*$ , is obtained by inverting Eq. (27) numerically.

The inflationary observables are then computed at  $\phi_*$ . The amplitude of scalar perturbations reads

$$A_s = \frac{U(\phi_*)}{24\pi^2 M_{\text{Pl}}^4 \epsilon(\phi_*)}, \quad (28)$$

while the scalar spectral index and the tensor-to-scalar ratio are given by

$$n_s = 1 - 6\epsilon(\phi_*) + 2\eta(\phi_*), \quad (29)$$

$$r = 16\epsilon(\phi_*). \quad (30)$$

In our analysis, for each choice of  $(n, y_D, M_D, M_N, y_N)$  we first determine the RG trajectory of  $\lambda(\mu)$ , construct the Einstein-frame potential  $U(\phi)$ , and then solve for the value of the non-minimal coupling  $\xi$  that reproduces the observed amplitude  $A_s \simeq 2.1 \times 10^{-9}$  at  $N_* = 55$ . The non-minimal coupling  $\xi$  is determined by requiring that the scalar amplitude matches the observed value given in Eq.(28). This condition is implemented by scanning  $\xi$  over a logarithmic range and identifying the value that satisfies the amplitude constraint. Once  $\xi$  is fixed, the inflationary observables  $n_s$  and  $r$  are evaluated at  $\phi_*(N)$ , corresponding to the number of e-folds in the range  $N \in [50, 60]$ . The resulting predictions in the  $(n_s, r)$  plane are then compared with the current constraints from Planck, WMAP, and BICEP/Keck [41].

### A. Inflationary Predictions in the $SM + (n)VLQ + RHN$ Framework

We first present the inflationary predictions of the SM extended with  $n$  degenerate down-type isosinglet VLQs and a right-handed neutrino (RHN) in the  $(n_s, r)$  plane for three benchmark VLQ masses,  $M_D = 1.5, 3.0, 5.0$  TeV, as shown in Fig.( 5). For each mass choice, we scan over the number of VLQs  $n$  and determine, for every  $(n, M_D)$ , the value of the non-minimal coupling  $\xi$  that reproduces the observed scalar amplitude  $A_s \simeq 2.1 \times 10^{-9}$  at  $N_* \simeq 55$  e-folds before the end of inflation. The resulting trajectories in the  $(n_s, r)$  plane exhibit two important features.

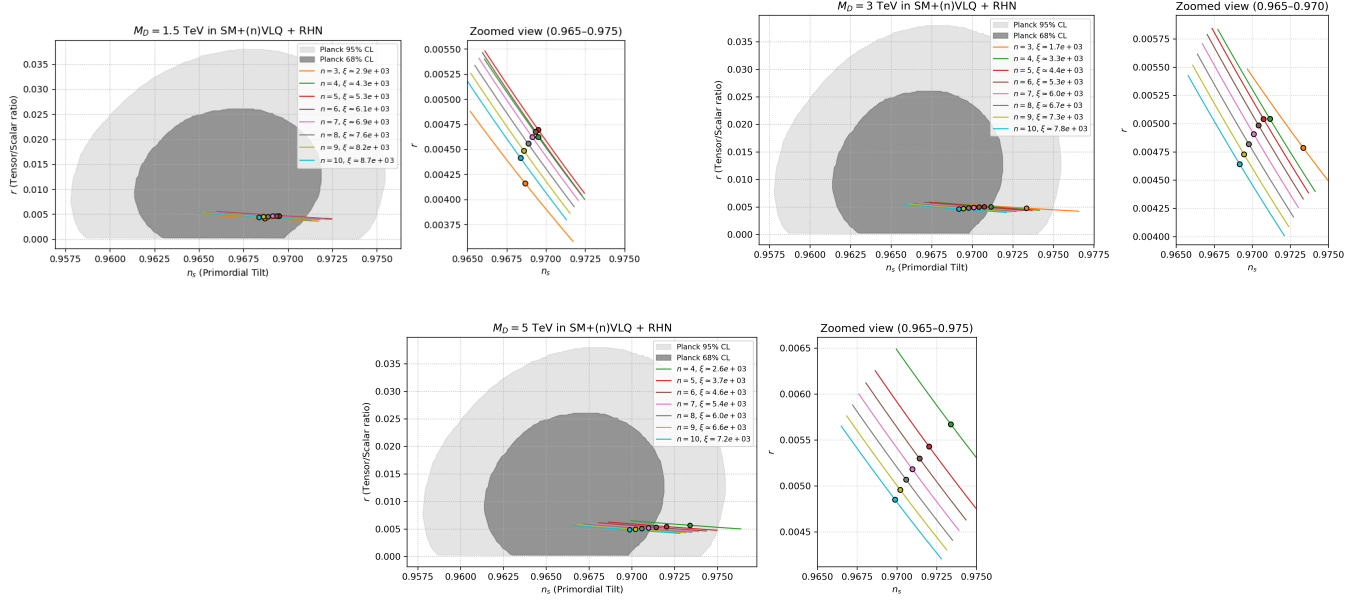


FIG. 5. Predictions for the spectral index  $n_s$  and tensor-to-scalar ratio  $r$  in the  $SM+(n)VLQ+RHN$  framework for benchmark VLQ masses  $M_D = 1.5, 3.0$ , and  $5.0$  TeV. Each coloured point corresponds to a different value of  $n$ , with the associated non-minimal coupling  $\xi$  determined by the CMB amplitude. The dark and light grey regions correspond to the 68% and 95% confidence contours from the combined Planck, WMAP, and BICEP/Keck analysis [41].

First, once the RHN is included, the points corresponding to different  $n$  and to the three benchmark values of  $M_D$  cluster very close to each other. In other words, the  $(n_s, r)$  predictions become only mildly sensitive to the number of VLQs and to their common mass. This behavior is a direct consequence of the RG-improved Higgs potential in the inflationary regime. In the  $SM + (n)VLQ + RHN$  model, the combined effect of the RHN Yukawa coupling and the VLQ sector renders the running of the Higgs quartic coupling  $\lambda(\mu)$  in the inflationary domain  $10^{15} - 10^{19}$  GeV remarkably smooth:  $\lambda(\mu)$  remains positive and its scale dependence is significantly suppressed. Since the slow-roll parameters  $\epsilon$  and  $\eta$  are determined by derivatives of the Einstein-frame potential Eq.(20), the small and weakly  $n$ -dependent slope of  $\lambda(\mu)$  in this region translates into very similar values of  $\epsilon_*$  and  $\eta_*$  for different  $(n, M_D)$ . The residual dependence on  $n$  and  $M_D$  is further absorbed by the  $A_s$  matching condition through a mild adjustment of  $\xi$ , which explains why the  $n_s$ - $r$  curves for the three benchmark masses lie close to one another.

Second, almost all points lie well within the region favored by the latest combined Planck, WMAP, and BICEP/Keck bounds [41], with a clear tendency toward the low- $r$  regime. This reflects the fact that the  $SM + (n)VLQ + RHN$  setup not only stabilizes the Higgs potential up to the Planck scale but also generates an inflationary plateau that is sufficiently flat to produce low tensor-to-scalar ratios and scalar tilts compatible with current CMB data. In summary, the RHN-induced smoothing of the RG-improved Higgs quartic in the inflationary range, together with the stabilizing VLQ contributions, leads to a set of  $n_s$ - $r$  predictions that are both theoretically well controlled and in excellent agreement with cosmological observations for all three benchmark values of  $M_D$ .

## B. Inflationary Predictions in the $SM + (n)VLQ$ Framework

Fig. 6 shows the predictions in the  $(n_s, r)$  plane for the  $SM+(n)VLQ$  model for three benchmark VLQ masses,  $M_D = 1.5, 3.0, 5.0$  TeV. For each mass choice, we scan over the VLQ multiplicity  $n$  and determine, for every  $(n, M_D)$ , the value of the non-minimal coupling  $\xi$  that reproduces the observed scalar amplitude  $A_s \simeq 2.1 \times 10^{-9}$  at  $N_* \simeq 55$  e-folds before the end of inflation. The resulting points are overlaid on the combined Planck, WMAP, and BICEP/Keck 68% and 95% confidence contours.

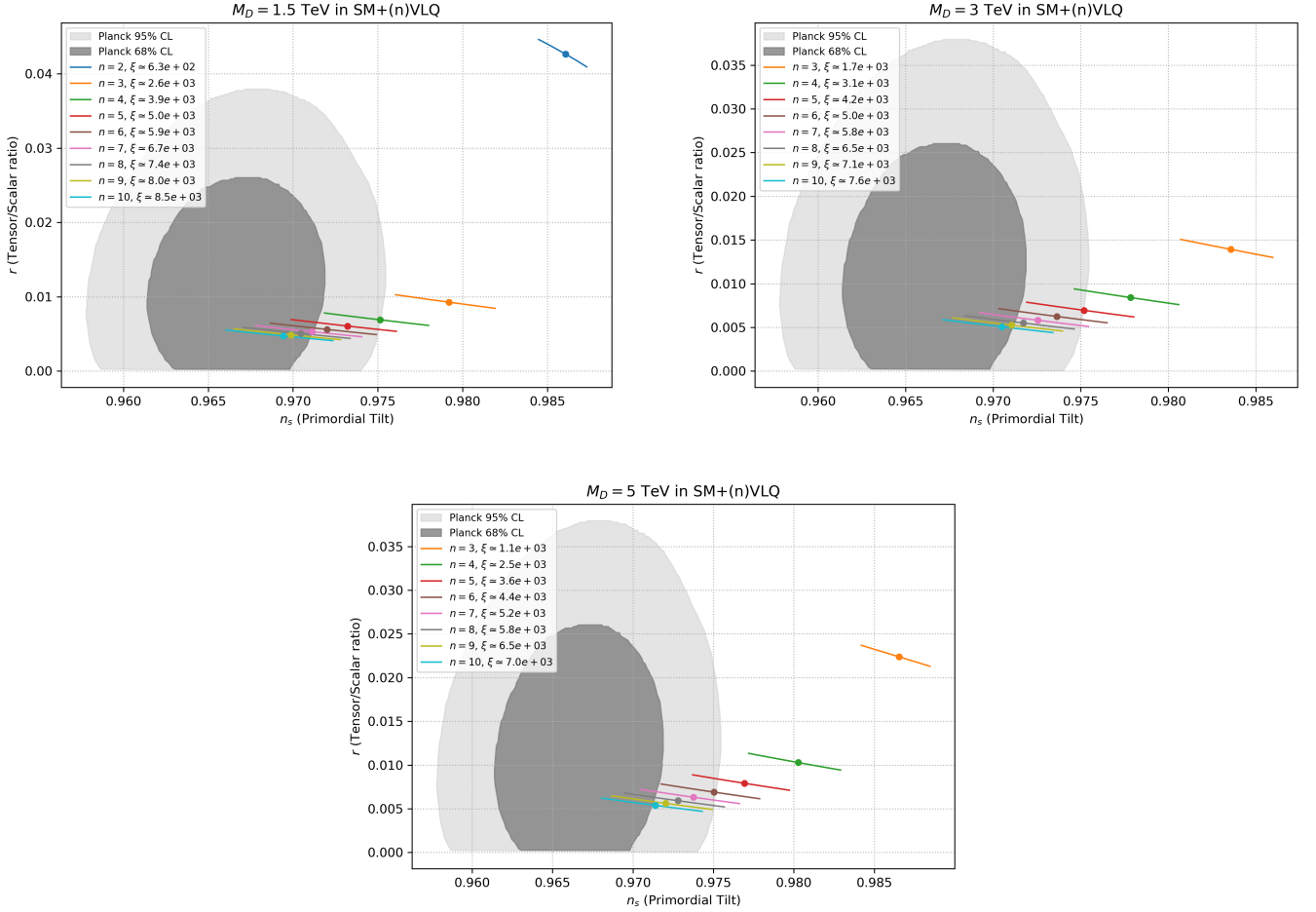


FIG. 6. Predictions for the spectral index  $n_s$  and tensor-to-scalar ratio  $r$  in the SM+( $n$ )VLQ framework for benchmark VLQ masses  $M_D = 1.5, 3.0$ , and  $5.0$  TeV. Each coloured point corresponds to a different value of  $n$ , with the associated non-minimal coupling  $\xi$  determined by the CMB amplitude. The dark and light grey regions correspond to the 68% and 95% confidence contours from the combined Planck, WMAP, and BICEP/Keck analysis [41]

In contrast to the SM+( $n$ )VLQ+RHN case, the SM+( $n$ )VLQ predictions exhibit a stronger dependence on both the number of VLQs  $n$  and the VLQ mass scale  $M_D$ . This behavior reflects the fact that, in the absence of the RHN, the running of the Higgs quartic coupling  $\lambda(\mu)$  in the inflationary regime,  $10^{15} - 10^{19}$  GeV, displays a stronger scale dependence, driven solely by the VLQ sector. As a consequence, the slow-roll parameters  $\epsilon_*$  and  $\eta_*$ , which depend on derivatives of the RG-improved Einstein-frame potential Eq.(20), vary more noticeably with  $(n, M_D)$ , leading to a broader spread of the corresponding  $(n_s, r)$  predictions. While a significant fraction of the points lies within the Planck+WMAP+BICEP/Keck allowed regions, some parameter choices—particularly for smaller values of  $n$  or specific  $M_D$ —lead to predictions that fall outside the Planck+WMAP+BICEP/Keck confidence regions. This contrasts with the SM+( $n$ )VLQ+RHN scenario, where the additional RHN Yukawa contribution further smooths the running of  $\lambda(\mu)$  and renders the inflationary observables only mildly sensitive to  $n$  and  $M_D$ . The comparison highlights the crucial role of the RHN in improving the overall agreement with CMB constraints by reducing the model dependence of the  $n_s$ – $r$  predictions.

## V. CONCLUSION

The primary goal of this work is to construct a phenomenologically minimal framework that simultaneously accounts for neutrino mass generation, electroweak vacuum stability, and Higgs inflation within a renormalizable extension of the Standard Model. To this end, we study a model containing  $n$  degenerate down-type isosinglet VLQs, supplemented by a single RHN implementing a Type-I seesaw mechanism. The analysis is carried out using the RG-improved Higgs

potential, where the running of the Higgs quartic coupling and the relevant inflationary dynamics are determined by solving the full set of RGEs, including the contributions from both the VLQs and RHN sectors.

We first consider the SM+ $(n)$ VLQ+RHN framework, in which the RHN simultaneously generates light neutrino masses via the Type-I seesaw mechanism and affects the RG evolution relevant for Higgs inflation. We find that, for suitable choices of  $n$  and  $M_{\mathcal{D}}$ , the combined effect of the VLQs and the RHN stabilizes the Higgs potential up to the Planck scale, while rendering the running of the Higgs quartic coupling remarkably smooth in the inflationary regime. As a consequence, the inflationary predictions in the  $(n_s, r)$  plane exhibit only a mild dependence on the number of VLQs,  $n$ , and the VLQ mass scale  $M_{\mathcal{D}}$ , with the resulting trajectories clustering in a narrow region that is mostly compatible with current CMB constraints.

For comparison, we also analyze the SM+ $(n)$ VLQ scenario by removing the RHN contributions from the RG equations. While the VLQs alone can still stabilize the Higgs potential and lead to viable Higgs inflation, the resulting inflationary observables display a stronger sensitivity to the VLQ parameters. This behavior manifests itself as a broader spread of predictions in the  $(n_s, r)$  plane, with certain parameter choices extending beyond the Planck+WMAP+BICEP/Keck confidence regions.

Overall, these results highlight the complementary roles of the VLQ and RHN sectors. The VLQs provide the dominant stabilizing effect on the Higgs potential, whereas the RHN plays a crucial role in smoothing the RG evolution in the inflationary domain and reducing the model dependence of the inflationary observables. Consequently, the SM+ $(n)$ VLQ+RHN framework emerges as a theoretically well-controlled and phenomenologically viable realization of Higgs inflation, consistent with electroweak vacuum stability and current cosmological data.

## ACKNOWLEDGMENT

This work is dedicated to the memory of Durmuş Demir, whose remarkable contributions to physics and enduring passion continue to be a source of inspiration. The author thanks Beste Korutlu Yılmaz and Ozan Sargin for valuable discussions related to electroweak vacuum stability and Higgs inflation.

## Appendix A: Renormalization Group Equations for the SM+ $(n)$ VLQ + RHN Model

In this appendix, we summarise the one-loop and (partially) two-loop RGEs used in the numerical analysis of the SM extended by  $n$  down-type VLQs and a single Majorana RHN.

The RG scale is defined as  $t = \ln \mu$ , and all  $\beta$  functions follow

$$\beta_x \equiv \frac{dx}{dt}. \quad (\text{A1})$$

### 1. Standard Model (1-loop)

At one loop the SM  $\beta$ -functions for the gauge couplings, top Yukawa and Higgs quartic coupling read [42]

$$\beta_{g_1}^{\text{SM},1\text{L}} = \frac{41}{10}g_1^3, \quad (\text{A2})$$

$$\beta_{g_2}^{\text{SM},1\text{L}} = -\frac{19}{6}g_2^3, \quad (\text{A3})$$

$$\beta_{g_3}^{\text{SM},1\text{L}} = -7g_3^3, \quad (\text{A4})$$

$$\beta_{y_t}^{\text{SM},1\text{L}} = y_t \left( \frac{9}{2}y_t^2 - 8g_3^2 - \frac{9}{4}g_2^2 - \frac{17}{20}g_1^2 \right), \quad (\text{A5})$$

$$\beta_{\lambda}^{\text{SM},1\text{L}} = 24\lambda^2 - 6y_t^4 + \frac{9}{8}g_2^4 + \frac{27}{200}g_1^4 + \frac{9}{20}g_2^2g_1^2 + \lambda \left( 12y_t^2 - 9g_2^2 - \frac{9}{5}g_1^2 \right). \quad (\text{A6})$$

## 2. Standard Model (2-loop top-sector terms)

We also include the dominant two-loop terms involving the top Yukawa, matching exactly the structure used in the numerical implementation [43]:

$$\beta_{g_1}^{\text{SM,2L}} = g_1^3 \left( \frac{199}{50} g_1^2 + \frac{27}{10} g_2^2 + \frac{44}{5} g_3^2 - \frac{17}{10} y_t^2 \right), \quad (\text{A7})$$

$$\beta_{g_2}^{\text{SM,2L}} = g_2^3 \left( \frac{9}{10} g_1^2 + \frac{35}{6} g_2^2 + 12 g_3^2 - \frac{3}{2} y_t^2 \right), \quad (\text{A8})$$

$$\beta_{g_3}^{\text{SM,2L}} = g_3^3 \left( \frac{11}{10} g_1^2 + \frac{9}{2} g_2^2 - 26 g_3^2 - 2 y_t^2 \right), \quad (\text{A9})$$

$$\begin{aligned} \beta_{y_t}^{\text{SM,2L}} = & -12 y_t^5 + y_t^3 \left( \frac{131}{16} g_2^2 + \frac{39}{80} g_1^2 + 15 g_3^2 \right) + y_t \left( \frac{3561}{15000} g_1^4 - \frac{27}{100} g_1^2 g_2^2 - \frac{23}{4} g_2^4 - \frac{57}{75} g_1^2 g_3^2 - 9 g_2^2 g_3^2 - 108 g_3^4 \right) \\ & + y_t \left( \frac{3}{2} \lambda^2 - 6 \lambda y_t^2 + \lambda \left( 3 g_2^2 + \frac{9}{25} g_1^2 \right) \right), \end{aligned} \quad (\text{A10})$$

$$\begin{aligned} \beta_{\lambda}^{\text{SM,2L}} = & -312 \lambda^3 + 36 \lambda^2 \left( 3 g_2^2 + \frac{3}{5} g_1^2 \right) - \lambda \left( \frac{73}{8} g_2^4 - \frac{351}{100} g_1^2 g_2^2 - \frac{16983}{5000} g_1^4 \right) + \frac{305}{8} g_2^6 - \frac{867}{200} g_1^2 g_2^4 - \frac{15093}{5000} g_1^4 g_2^2 - \frac{92097}{125000} g_1^6 \\ & - 3 \lambda y_t^4 + 30 y_t^6 - y_t^4 \left( \frac{8}{5} g_1^2 + 8 g_2^2 + 32 g_3^2 \right) + \lambda y_t^2 \left( \frac{45}{2} g_2^2 + \frac{17}{2} g_1^2 + 80 g_3^2 - 144 y_t^2 \right). \end{aligned} \quad (\text{A11})$$

## 3. Down-type singlet VLQ contributions (1 loop)

In the following, we present the RGE for  $y_D$  together with the corresponding one-loop contributions relevant for the present analysis [24, 25].

$$\beta_{y_D}^{\text{VLQ}} = y_D \left[ \frac{3}{2} y_t^2 + \left( \frac{3}{2} + 3n \right) y_D^2 - 8 g_3^2 - \frac{9}{4} g_2^2 - \frac{1}{4} g_1^2 \right], \quad (\text{A12})$$

$$\Delta \beta_{g_1}^{\text{VLQ}} = \frac{4}{15} n g_1^3, \quad (\text{A13})$$

$$\Delta \beta_{g_2}^{\text{VLQ}} = 0, \quad (\text{A14})$$

$$\Delta \beta_{g_3}^{\text{VLQ}} = \frac{2}{3} n g_3^3, \quad (\text{A15})$$

$$\Delta \beta_{y_t}^{\text{VLQ}} = \frac{3}{2} n y_D^2 y_t, \quad (\text{A16})$$

$$\Delta \beta_{\lambda}^{\text{VLQ}} = -6n y_D^4 + 12n y_D^2 \lambda. \quad (\text{A17})$$

## 4. Majorana RHN contributions (1 loop)

In the following, we present the RGE for the RHN Yukawa coupling and retain only its dominant one-loop contributions to the Higgs quartic coupling, which are sufficient to capture the impact of the RHN sector on vacuum stability. [44, 45]

$$\beta_{y_N}^{\text{RHN}} = y_N \left( \frac{5}{2} y_N^2 + 3n y_D^2 + 3 y_t^2 - \frac{9}{20} g_1^2 - \frac{9}{4} g_2^2 \right), \quad (\text{A18})$$

$$\Delta \beta_{\lambda}^{\text{RHN}} = -2 y_N^4 + 4 y_N^2 \lambda. \quad (\text{A19})$$

### 5. Full RG system in the $SM + (n)VLQ + RHN$ Framework

In this part, we summarize the RGEs for the couplings in the  $SM + (n)VLQ + RHN$  framework. Collecting all contributions, the full  $\beta$ -functions used in the numerical analysis read

$$\beta_{g_1} = \frac{1}{16\pi^2} \beta_{g_1}^{\text{SM},1\text{L}} + \frac{1}{(16\pi^2)^2} \beta_{g_1}^{\text{SM},2\text{L}} + \frac{1}{16\pi^2} \Delta\beta_{g_1}^{\text{VLQ}}, \quad (\text{A20})$$

$$\beta_{g_2} = \frac{1}{16\pi^2} \beta_{g_2}^{\text{SM},1\text{L}} + \frac{1}{(16\pi^2)^2} \beta_{g_2}^{\text{SM},2\text{L}}, \quad (\text{A21})$$

$$\beta_{g_3} = \frac{1}{16\pi^2} \beta_{g_3}^{\text{SM},1\text{L}} + \frac{1}{(16\pi^2)^2} \beta_{g_3}^{\text{SM},2\text{L}} + \frac{1}{16\pi^2} \Delta\beta_{g_3}^{\text{VLQ}}, \quad (\text{A22})$$

$$\beta_{y_t} = \frac{1}{16\pi^2} \beta_{y_t}^{\text{SM},1\text{L}} + \frac{1}{(16\pi^2)^2} \beta_{y_t}^{\text{SM},2\text{L}} + \frac{1}{16\pi^2} \Delta\beta_{y_t}^{\text{VLQ}}, \quad (\text{A23})$$

$$\beta_\lambda = \frac{1}{16\pi^2} \beta_\lambda^{\text{SM},1\text{L}} + \frac{1}{(16\pi^2)^2} \beta_\lambda^{\text{SM},2\text{L}} + \frac{1}{16\pi^2} \Delta\beta_\lambda^{\text{VLQ}} + \frac{1}{16\pi^2} \Delta\beta_\lambda^{\text{RHN}}, \quad (\text{A24})$$

$$\beta_{y_D} = \frac{1}{16\pi^2} \beta_{y_D}^{\text{VLQ}}, \quad (\text{A25})$$

$$\beta_{y_N} = \frac{1}{16\pi^2} \beta_{y_N}^{\text{RHN}}. \quad (\text{A26})$$

The RGEs for the  $SM + (n)VLQ$  framework are obtained by removing all right-handed-neutrino contributions from the above equations.

### Appendix B: Input Values at the Top-Quark Mass Scale

For the numerical solution of the RGEs, all SM couplings are initialized at the top-quark mass scale  $\mu = m_t$ . Unless stated otherwise, we adopt the central values reported by the Particle Data Group (PDG) [46] and widely used in vacuum-stability analyses. The input parameters employed throughout this work are summarized in Table I.

TABLE I. Input values for the SM parameters at  $\mu = m_t$ , which serve as boundary conditions for the RG evolution discussed in the main text, together with the initial conditions for the RHN and VLQ parameters defined at their respective mass thresholds.

Parameter	Value
Higgs mass	$m_h = 125.10 \text{ GeV}$
Top-quark mass	$m_t = 172.7 \text{ GeV}$
Strong coupling	$\alpha_s(m_Z) = 0.1181$
Gauge coupling $g_1$ (GUT-normalized)	$g_1(m_t) = 0.462$
Gauge coupling $g_2$	$g_2(m_t) = 0.647$
Gauge coupling $g_3$	$g_3(m_t) = 1.166$
Top Yukawa coupling	$y_t(m_t) = 0.936$
Higgs quartic coupling	$\lambda(m_t) = 0.126$
RHN mass	$M_N = 10^{14} \text{ GeV}$
RHN Yukawa coupling	$y_N(M_N) = 0.42$
VLQ Dirac mass	$M_D = 1.5, 3.0, 5.0 \text{ TeV}$
VLQ Yukawa coupling	$y_D(M_D) = 0.15$
Number of VLQs	$n = 1 - 10$

---

[1] Q. R. Ahmad *et al.* [SNO Collaboration], “Measurement of the Rate of  $\nu_e + d \rightarrow p + p + e^-$  Interactions Produced by  ${}^8\text{B}$  Solar Neutrinos at the Sudbury Neutrino Observatory,” Phys. Rev. Lett. **87**, 071301 (2001), [arXiv:nucl-ex/0106015].

[2] Y. Fukuda *et al.* [Super-Kamiokande Collaboration], “Evidence for Oscillation of Atmospheric Neutrinos,” Phys. Rev. Lett. **81**, 1562–1567 (1998), [arXiv:hep-ex/9807003].

- [3] G. Degrassi et al., “Higgs mass and vacuum stability in the Standard Model at NNLO,” *JHEP* **08**, 098 (2012), [arXiv:1205.6497 [hep-ph]].
- [4] D. Buttazzo et al., “Investigating the near-criticality of the Higgs boson,” *JHEP* **12**, 089 (2013), [arXiv:1307.3536 [hep-ph]].
- [5] A. A. Starobinsky, “A New Type of Isotropic Cosmological Models Without Singularity,” *Phys. Lett. B* **91**, 99 (1980). doi:10.1016/0370-2693(80)90670-X.
- [6] F. L. Bezrukov and M. Shaposhnikov, “The Standard Model Higgs boson as the inflaton,” *Phys. Lett. B* **659**, 703 (2008), [arXiv:0710.3755 [hep-th]].
- [7] P. Minkowski, “ $\mu \rightarrow e\gamma$  at a Rate of One Out of  $10^9$  Muon Decays?”, *Phys. Lett. B* **67**, 421–428 (1977), doi:10.1016/0370-2693(77)90435-X.
- [8] M. Gell-Mann, P. Ramond, and R. Slansky, “Complex Spinors and Unified Theories,” in *Supergavity*, edited by P. van Nieuwenhuizen and D. Z. Freedman (North Holland, Amsterdam, 1979), p. 315 [arXiv:1306.4669 [hep-th]].
- [9] T. Yanagida, in *Proceedings of the Workshop on Unified Theory and the Baryon Number of the Universe*, edited by O. Sawada and A. Sugamoto (KEK, Tsukuba, 1979).
- [10] R. N. Mohapatra and G. Senjanović, “Neutrino Mass and Spontaneous Parity Nonconservation,” *Phys. Rev. Lett.* **44**, 912 (1980), doi:10.1103/PhysRevLett.44.912.
- [11] T. P. Cheng and L. F. Li, “Neutrino Masses, Mixings and Oscillations in  $SU(2) \times U(1)$  Models of Electroweak Interactions,” *Phys. Rev. D* **22**, 2860 (1980), doi:10.1103/PhysRevD.22.2860.
- [12] R. N. Mohapatra and G. Senjanović, “Neutrino masses and mixings in gauge models with spontaneous parity violation,” *Phys. Rev. D* **23**, 165 (1981), doi:10.1103/PhysRevD.23.165.
- [13] R. Foot, H. Lew, X. G. He and G. C. Joshi, “Seesaw Neutrino Masses Induced by a Triplet of Leptons,” *Z. Phys. C* **44**, 441–444 (1989), doi:10.1007/BF01415558.
- [14] D. Demir, C. Karahan and O. Sargin, “Type-3/2 seesaw mechanism,” *Phys. Rev. D* **104**, no.7, 075038 (2021), [arXiv:2105.06539 [hep-ph]].
- [15] M. Sher, “Electroweak Higgs Potentials and Vacuum Stability,” *Phys. Rept.* **179**, 273–418 (1989), doi:10.1016/0370-1573(89)90061-6.
- [16] K. G. Chetyrkin and M. F. Zoller, “Three-loop beta functions for the Higgs self-interaction and the top-Yukawa coupling,” *JHEP* **06**, 033 (2012), [arXiv:1205.2892 [hep-ph]].
- [17] M. Gonderinger, Y. Li, H. Patel and M. J. Ramsey-Musolf, “Vacuum Stability, Perturbativity, and Scalar Singlet Dark Matter,” *JHEP* **01**, 053 (2010), [arXiv:0910.3167 [hep-ph]].
- [18] P. Ghorbani, “Vacuum stability vs. positivity in real singlet scalar extension of the standard model,” *Nucl. Phys. B* **971**, 115533 (2021), [arXiv:2104.09542 [hep-ph]].
- [19] Z. Péli and Z. Trócsányi, “Vacuum stability and scalar masses in the superweak extension of the Standard Model,” *Phys. Rev. D* **106**, 055045 (2022), [arXiv:2204.07100 [hep-ph]].
- [20] G. Hiller, T. Höhne, D. F. Litim and T. Steudtner, “Vacuum Stability in the Standard Model and Beyond,” *Phys. Rev. D* **110**, 115017 (2024), [arXiv:2401.08811 [hep-ph]].
- [21] W. Rodejohann and H. Zhang, “Impact of massive neutrinos on the Higgs self-coupling and electroweak vacuum stability,” *JHEP* **06**, 022 (2012), [arXiv:1203.3825 [hep-ph]].
- [22] A. Datta, A. Elsayed, S. Khalil and A. M. Moretti, “Higgs vacuum stability in the  $B - L$  extended Standard Model,” *Phys. Rev. D* **88**, 053011 (2013), [arXiv:1308.0816 [hep-ph]].
- [23] S. Oda, N. Okada and D. s. Takahashi, ‘Classically conformal  $U(1)'$  extended standard model and Higgs vacuum stability,” *Phys. Rev. D* **92**, no.1, 015026 (2015), [arXiv:1504.06291 [hep-ph]].
- [24] S. Gopalakrishna and A. Velusamy, “Higgs vacuum stability with vectorlike fermions,” *Phys. Rev. D* **99**, 115020 (2019), [arXiv:1812.11303 [hep-ph]].
- [25] A. Arsenault, K. Y. Cingiloglu and M. Frank, “Vacuum stability in the Standard Model with vector-like fermions,” *Phys. Rev. D* **107**, 036018 (2023), [arXiv:2207.10332 [hep-ph]].
- [26] R. N. Lerner and J. McDonald, “Gauge singlet scalar as inflaton and thermal relic dark matter,” *Phys. Rev. D* **80**, 123507 (2009), [arXiv:0909.0520 [hep-ph]].
- [27] K. Nakayama and F. Takahashi, “Running kinetic inflation,” *JCAP* **1011**, 009 (2010), [arXiv:1008.2956 [hep-ph]].
- [28] A. O. Barvinsky, A. Y. Kamenshchik and A. A. Starobinsky, “Inflation scenario via the Standard Model Higgs boson and LHC,” *JCAP* **11**, 021 (2008), [arXiv:0809.2104 [hep-ph]].
- [29] F. Bauer and D. A. Demir, “Inflation with Non-Minimal Coupling: Metric versus Palatini Formulations,” *Phys. Lett. B* **665**, 222–226 (2008), [arXiv:0803.2664 [hep-ph]].
- [30] J. Rubio, “Higgs inflation,” *Front. Astron. Space Sci.* **5**, 50 (2019), [arXiv:1807.02376 [hep-ph]].
- [31] R. L. Workman *et al.* (Particle Data Group), “Review of particle physics,” *Prog. Theor. Exp. Phys.* 2022, 083C01 (2022), doi:10.1093/ptep/ptac097.
- [32] P. F. De Salas, S. Gariazzo, O. Mena, C. A. Ternes and M. Tórtola, “Neutrino Mass Ordering from Oscillations and Beyond: 2018 Status and Future Prospects,” *Front. Astron. Space Sci.* **5**, 36 (2018), [arXiv:1806.11051 [hep-ph]].
- [33] M. Aaboud *et al.* [ATLAS], “Search for pair production of heavy vector-like quarks decaying into high- $p_T$   $W$  bosons and top quarks in the lepton-plus-jets final state in  $pp$  collisions at  $\sqrt{s} = 13$  TeV with the ATLAS detector,” *JHEP* **08**, 048 (2018), [arXiv:1806.01762 [hep-ex]].
- [34] A. Tumasyan *et al.* [CMS], “Search for pair production of vector-like quarks in leptonic final states in proton-proton collisions at  $\sqrt{s} = 13$  TeV,” *JHEP* **07**, 020 (2023), [arXiv:2209.07327 [hep-ex]].
- [35] C. Y. Chen, S. Dawson and E. Furlan, “Vectorlike fermions and Higgs effective field theory revisited,” *Phys. Rev. D* **96**, no.1, 015006 (2017), [arXiv:1703.06134 [hep-ph]].

- [36] J. A. Aguilar-Saavedra, R. Benbrik, S. Heinemeyer and M. Pérez-Victoria, “Handbook of vectorlike quarks: Mixing and single production,” Phys. Rev. D **88**, no.9, 094010 (2013), [arXiv:1306.0572 [hep-ph]].
- [37] L. Lavoura and J. P. Silva, “Bounds on the mixing of the down-type quarks with vectorlike singlet quarks,” Phys. Rev. D **47**, 1117 (1993), doi:10.1103/PhysRevD.47.1117.
- [38] A. Adhikary, M. Olechowski, J. Rosiek and M. Ryczkowski, “Theoretical constraints on models with vectorlike fermions,” Phys. Rev. D **110**, 075029 (2024), [arXiv:2406.16050 [hep-ph]].
- [39] D. A. Dicus and V. S. Mathur, “Upper bounds on the values of masses in unified gauge theories,” Phys. Rev. D **7**, 3111 (1973), doi:10.1103/PhysRevD.7.3111.
- [40] M. S. Chanowitz, M. A. Furman and I. Hinchliffe, “Weak Interactions of Ultraheavy Fermions. 2.,” Nucl. Phys. B **153**, 402-430 (1979), doi:10.1016/0550-3213(79)90606-0.
- [41] P. A. R. Ade *et al.* [BICEP and Keck], “Improved Constraints on Primordial Gravitational Waves using Planck, WMAP, and BICEP/Keck Observations through the 2018 Observing Season,” Phys. Rev. Lett. **127**, no.15, 151301 (2021), [arXiv:2110.00483 [astro-ph.CO]].
- [42] T. P. Cheng and L. F. Li, *Gauge Theory of Elementary Particle Physics*, Oxford University Press (1984).
- [43] M.E. Machacek and M.T. Vaughn, “Two-loop Renormalization Group Equations in a General Quantum Field Theory (I). Gauge Fields”, Nucl. Phys. B222 (1983) 83, doi:10.1016/0550-3213(83)90610-7.
- [44] S. Antusch, M. Drees, J. Kersten, M. Lindner and M. Ratz, “Neutrino mass operator renormalization revisited,” Phys. Lett. B **519**, 238-242 (2001), [arXiv:hep-ph/0108005 [hep-ph]].
- [45] S. Antusch, M. Drees, J. Kersten, M. Lindner and M. Ratz, “Neutrino mass operator renormalization in two Higgs doublet models and the MSSM,” Phys. Lett. B **525**, 130-134 (2002), [arXiv:hep-ph/0110366 [hep-ph]].
- [46] S. Navas *et al.* (Particle Data Group), “Review of Particle Physics,” Phys. Rev. D **110**, 030001 (2024), doi:10.1103/PhysRevD.110.030001.